

SEISMIC RESPONSE OF NONLINEAR CONTROLLED ISOLATED BRIDGES UNDER NEAR-FIELD GROUND MOTIONS

T.Y. Lee¹⁾, and K. Kawashima²⁾

1) Graduate Student, Department of Civil Engineering, Tokyo Institute of Technology, Japan

2) Professor, Department of Civil Engineering, Tokyo Institute of Technology, Japan

tylee@cv.titech.ac.jp, kawasima@cv.titech.ac.jp

Abstract: Seismic isolation has been extensively used worldwide for bridges. Considerable progress has been made in control method of civil engineering structures subjected to environmental loads in the past two decades. However, in most studies, structures except isolators are assumed to be linear elastic. This paper shows the efficiency of supplementary dampers with active control algorithm to mitigate the large deck displacement and the hysteretic behavior of column. Magnetorheological dampers (MR-dampers) are used in this numerical analysis so that arbitrary control algorithm for damping force vs. bridge response relations is introduced. Both external and internal damper allocations are implemented to evaluate the difference of performance.

1. INTRODUCTION

Seismic isolation has been extensively used worldwide for bridges. However isolated bridges inherently exhibit inelastic responses and excessive deck displacements when subjected to a strong near-field ground motion, such as Northridge Earthquake in USA, 1994, Kobe Earthquake in Japan, 1995 and Chi-Chi Earthquake in Taiwan, Duzce Earthquake in Turkey, 1999. Such large displacements enhance the difficulty of design of bridge accessory equipments, such as expansion joints and unseating prevention devices, and may affect the recovery and reconstruction after earthquakes even though collapse does not occur.

This paper shows the efficiency of supplementary dampers to mitigate the large deck displacement and the hysteretic behavior of columns. Magnetorheological (MR) fluid dampers are used in this analysis so that arbitral control algorithm for damping force vs. bridge response relations is introduced. A bridge is composed of low-damping isolation bearings and MR dampers, and it is subjected to five near-field ground motions. Both external and internal damper allocations are implemented by numerical simulation based on active optimum control with full-state feedback to evaluate their efficiency.

In most control studies, structures except isolators are assumed to be linear elastic even under strong earthquakes. However, based on the modern bridge seismic design method, bridge columns exhibit high hysteresis to dissipate more energy. In this study, hysteretic behaviors of columns are included in the analysis as well. It is found from the analysis that columns with high ductility still exhibit hysteretic behavior under extreme earthquakes and the efficiency of control force due to classical control method is not as remarkable as the one with low ductility under moderate earthquakes.

2. ISOLATED BRIDGES WITH SUPPLEMENTARY DAMPERS

Consider a n degrees of freedom nonlinear or hysteretic structure subjected to a one-dimensional earthquake horizontal ground acceleration $\ddot{x}_g(t)$. The equation of motion is given by

$$\mathbf{M} \ddot{\mathbf{u}}(t) + \mathbf{F}_D[\dot{\mathbf{u}}(t)] + \mathbf{F}_S[\mathbf{u}(t)] = \boldsymbol{\eta} \ddot{x}_g(t) + \mathbf{H}^T \mathbf{U}(t) \quad (1)$$

in which $\mathbf{u}(t) = [u_1, u_2, \dots, u_n]^T$ is an n -vector with u_i being the displacement of the i th element; \mathbf{M} is a $(n \times n)$ mass vector. $\mathbf{F}_D[\dot{\mathbf{u}}(t)]$ and $\mathbf{F}_S[\mathbf{u}(t)]$ are nonlinear damping and stiffness vectors, respectively; $\mathbf{U}(t)$ is a r -dimensional consisting of r active control damping forces from the MR dampers, and \mathbf{H} is a $(n \times r)$ denotes the location of MR dampers. In this paper, a prime indicates the transpose of either a matrix or a vector.

In the state space, Eq. (1) can be expressed as

$$\dot{\mathbf{Z}}(t) = \mathbf{g}[\mathbf{Z}(t)] + \mathbf{B} \mathbf{U}(t) + \mathbf{W} \ddot{x}_g(t) \quad (2)$$

in which $\mathbf{g}[\mathbf{Z}(t)]$ is a $2n$ -vector which is a nonlinear function of the state vector $\mathbf{Z}(t)$ and other matrices are defined as follows:

$$\mathbf{Z}(t) = \begin{bmatrix} \mathbf{u}(t) \\ \dot{\mathbf{u}}(t) \end{bmatrix}; \quad \mathbf{g}[\mathbf{Z}(t)] = \begin{bmatrix} \dot{\mathbf{u}}(t) \\ -\mathbf{M}^{-1}[\mathbf{F}_D + \mathbf{F}_S] \end{bmatrix}; \quad \mathbf{B} = \begin{bmatrix} 0 \\ \mathbf{M}^{-1}\mathbf{H} \end{bmatrix}; \quad \mathbf{W} = \begin{bmatrix} 0 \\ \mathbf{M}^{-1}\boldsymbol{\eta} \end{bmatrix} \quad (3)$$

The LQR performance index is given by

$$J = \int_0^{t_f} [\mathbf{Z}'(t)\mathbf{Q}\mathbf{Z}(t) + \mathbf{U}'(t)\mathbf{R}\mathbf{U}(t)]dt \quad (4)$$

in which \mathbf{Q} is a $(2n \times 2n)$ symmetric positive semidefinite weighting matrix and \mathbf{R} is a positive weighting matrix.

Referring to the generalization of optimal control theory for nonlinear structures by Yang et al. (1994), minimizing the objective function, J , given by Eq. (4) subjected to the constraint of the state equation of motion, Eq. (2) yields the control damping force as follows:

$$\mathbf{U}(t) = -0.5\mathbf{R}^{-1}\mathbf{B}\mathbf{P}\mathbf{Z}(t) \quad (5)$$

$$\boldsymbol{\Lambda}_0^T \mathbf{P} + \mathbf{P}\boldsymbol{\Lambda}_0 - 0.5\mathbf{P}\mathbf{B}\mathbf{R}^{-1}\mathbf{B}^T \mathbf{P}\mathbf{Z}(t) = -2\mathbf{Q} \quad (6)$$

in which \mathbf{P} is the Riccati matrix where

$$\boldsymbol{\Lambda}_0 = \partial \mathbf{g}(\mathbf{Z}) / \partial \mathbf{Z} |_{\mathbf{Z}=0} \quad (7)$$

Note that Eq. (6) is approximated by neglecting the earthquake ground acceleration $\ddot{x}_g(t)$ and linearizing the structural system at the initial equilibrium point $\mathbf{Z}=0$. Since the term $\mathbf{P}\mathbf{B}\mathbf{R}^{-1}\mathbf{B}^T \mathbf{P}$ is positive semidefinite, Eq. (7) can be approximated further by

$$\boldsymbol{\Lambda}_0^T \mathbf{P} + \mathbf{P}\boldsymbol{\Lambda}_0 = -2\mathbf{Q} \quad (8)$$

which is known as the Lyapunov equation.

The bridge structure and isolated bearing may be idealized to be nonlinear or hysteretic. The following hysteretic model is used for both the bridge structure and isolator. The stiffness restoring

force is given by Bouc-Wen model.

$$F_{si}(t) = \alpha_i k_i x_i(t) + (1 - \alpha_i) k_i x_{yi} v_i \quad (9)$$

in which x_i = deformation of the i th element, k_i = elastic stiffness, α_i = ratio of the post-yielding to pre-yielding stiffness, x_{yi} = yielding deformation, and v_i = hysteretic variable with $|v_i| \leq 1$, where

$$\dot{x}_i = x_{yi}^{-1} \left[A_i \dot{x}_i - \beta_i |\dot{x}_i| |v_i|^{n_i-1} v_i - \gamma_i \dot{x}_i |v_i|^{n_i} \right] \quad (10)$$

in which parameters A_i , β_i , γ_i and n_i govern the scale, general shape and smoothness of the hysteresis loop. Note that the i th element is linear elastic if $\alpha_i = 1$.

3. NUMERICAL SIMULATION

A target bridge with isolators is considered as shown in Fig. 1. MR dampers are installed between the deck and the column or the deck and the abutment. When MR dampers are connected to the abutment, they are regarded as applying external force to the bridge. On the other hand, when MR dampers are connected to the deck, the damping forces are regarded as part of internal forces. The effectiveness of both allocations will be discussed respectively. Assuming that the soil is stiff, the response of bridge may be idealized as a two degree of freedom system as shown in Fig. 2. The mass of deck and column are 700T and 140T, respectively. The columns exhibit bilinear elastoplastic behavior with zero post-yield stiffness, whereas the isolator is elastomeric with low damping, Fig.3. The fundamental natural period of the entire bridge is 1.3 second. For simplicity, the damping of the system is considered as linear viscous damping and the damping ratio of 2% is assumed for the both modal shapes.

The earthquake records used in this study are JMA Kobe Observatory and JR-Takatori Station in the 1995 Kobe Earthquake, Japan, Duzce in the 1999 Duzce Earthquake, Turkey, Sylmar Parking Lot in the 1994 Northridge, USA, and Sun-Moon Lake in 1999 Chi-Chi Earthquake, Taiwan, as shown in Fig. 4. All the excitations are applied at the full intensity for the evaluation of the performance indices.

With the MR damper applying the control force to the bridge, the structural response depends on the weighting matrices \mathbf{Q} and \mathbf{R} . For this example, the \mathbf{Q} matrix is considered as a diagonal matrix with all the diagonal elements equal to 1.0. Since the \mathbf{R} weighting matrix consists of only one element and the magnitude of required control damping force mainly depends on \mathbf{R} value, \mathbf{R} value is implemented over a wide range in order to evaluate and search for the suitable \mathbf{R} value under the feasible capacity of devices. In some studies, considering that the required control force may be too large when the earthquake excitation is strong, saturated controller is adopted to bound the control force. In this study, control force will not be limited but only control force below 30% of deck weight is evaluated.

Time histories of all the response quantities have been computed within 30 seconds of the records except Chi-Chi Earthquake with 40 seconds. The generated control damping force, and the corresponding displacement and absolute acceleration of deck and column are evaluated using normalized indices. The performance index of generated control damping force is normalized by the deck weight. The performance indices of displacement and absolute acceleration are normalized by the corresponding magnitudes in the uncontrolled structure. The results of the evaluations for external damper and internal damper are presented as follows.

3.1 External damper

Time history displacement responses for JMA Kobe and Sun-Moon Lake earthquakes with \mathbf{R} of

5×10^{-12} are shown in Figs. 5 and 6. The hysteretic loops of the column and isolator are also shown in Figs. 7 and 8. The corresponding stroke and damping force hystereses of the MR damper are shown in Fig. 9. As observed from the results, displacement responses are reduced substantially from the uncontrolled responses. The column even exhibits elastic response using controlled damper under JMA Kobe record, while column displacement ductility factor decreases from 12 to 7 under Sun-Moon Lake record.

The performance indices described above with respect to weighting \mathbf{R} for five ground motions are shown in Fig. 10. The column displacement ductility factor without control is 4.1, 3.8 and 1.1 under JMA Kobe, Duzce and Sylmar records, respectively, while it is 9.2 and 11.8 under JR-Takatori and Sun-Moon Lake records, respectively, which are not shown in Fig. 10(d). The higher ductility factor in uncontrolled bridge, the higher control damping force is generated as shown in Fig. 10(a). However, even though higher control force is applied, the deck displacement under Sun-Moon Lake and JR-Takatori do not reduce to the level developed under other records except Sylmar, as shown in Figs. 10(b), and it is important to note that column still exhibits high inelastic behavior as shown in Fig. 10(d). One can attribute it to the insufficient assumption in the linearization of the bridge that the initial stiffness is used to determine the gain vector of control force.

3.2 Internal damper

Time history displacement responses of the deck and the column under JMA Kobe and Sun-Moon Lake records with \mathbf{R} of 5×10^{-12} are shown in Figs. 11 and 12. The hysteretic loops of the column and isolator are also shown in Figs. 13 and 14. The corresponding stroke and damping force hystereses of the MR damper are shown in Fig. 15. Using the controlled damper, both the deck and column displacements can be decreased, but still some inelastic deformation occurs in the column.

The performance indices with respect to weighting \mathbf{R} for five ground motions are shown in Fig. 16. As same as the external damper, the deck displacement under Sun-Moon Lake and JR-Takatori do not reduce to the level developed under other records as shown in Figs. 16(b) even though higher control force is applied as shown in Fig. 16(a). One can also attribute it to the insufficient assumption in the linearization of the bridge that the initial stiffness is used to determine the gain vector of control force. Note that column still exhibits hysteretic behavior compared to the same level of control force applied by the external damper under all ground motions except Sylmar as shown in Fig. 16(d). In addition, the decrease of deck and column displacements results in an increase of deck accelerations because the internal damping force restricts the relative displacement between the deck and the column as shown in Fig. 16(e).

4. CONCLUSIONS

The feasibility and effectiveness of MR dampers for controlling the seismic response of isolated bridges have been evaluated by numerical simulations under five strong near-field ground motions. The damper allocations investigated include the external damper and the internal damper. The following conclusions may be obtained from the results presented herein.

- (a) Both damper allocations are effective for active control in reducing the deck displacement subjected to the near-field ground motions. Especially, the external damper shows higher efficacy than the internal damper and no penalty of increasing deck acceleration. However the external damper may only be installed at the ends of bridges such as abutments. It is limited for wider application in seismic design.
- (b) The magnitude of damper force required for control depends on not only the weighting \mathbf{R} but also the intensity and characteristic of ground excitation. In addition, the performance indices extensively vary depending on ground motions so that one should pay an attention on the type

of ground motions to maintain the stability of control.

- (c) Under the control using a feasible level of damping force, the amount of mitigation of the deck displacement and the plastic deformation in the column is insufficient. Further improvement of the control method that can be applied to bridges with high nonlinearity is required.

Acknowledgements:

The authors acknowledge support from the Center for Urban Earthquake Engineering (CUEE) in Tokyo Institute of Technology.

References:

Kawashima, K. and Unjoh, S. (1994), "Seismic Response Control of Bridges by Variable dampers," *Journal of Structural Engineering*, American Society of Civil Engineers, **120**(9), 2583-2601.
 Yang, J.N., Li, Z. and Vongchavallitkul, S. (1994), "A Generalization of Optimal Control Theory: Linear and Nonlinear Control," *Journal of Engineering Mechanics*, American Society of Civil Engineers, **120**(2), 266-283.
 Yang, J.N., Wu, J.C., Kawashima, K. and Unjoh, S. (1995), "Hybrid Control of Seismic-excited bridge structures," *Earthquake Engineering and Structural Dynamics*, **24**(11), 1437-1451.

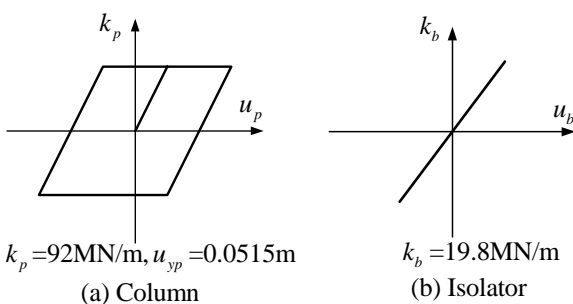
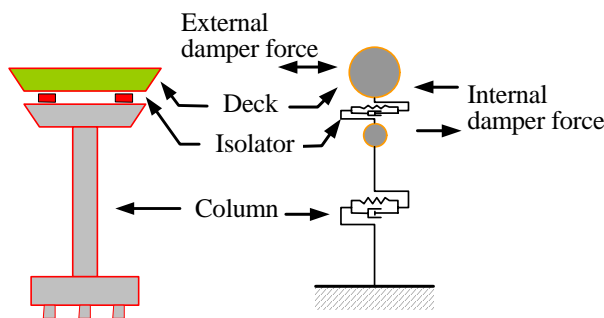
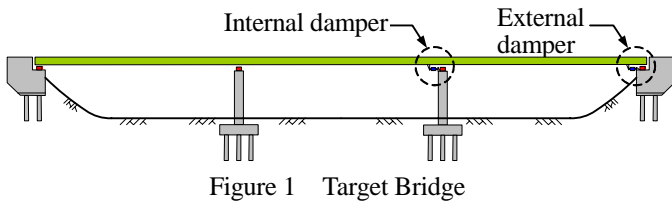


Figure 3 Material Behavior of Column and Isolator

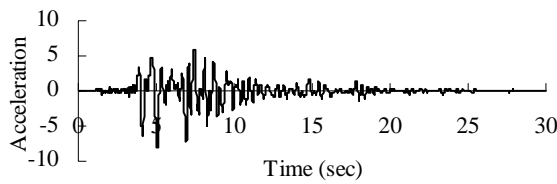


Figure 4 Ground Motions (m/sec²)

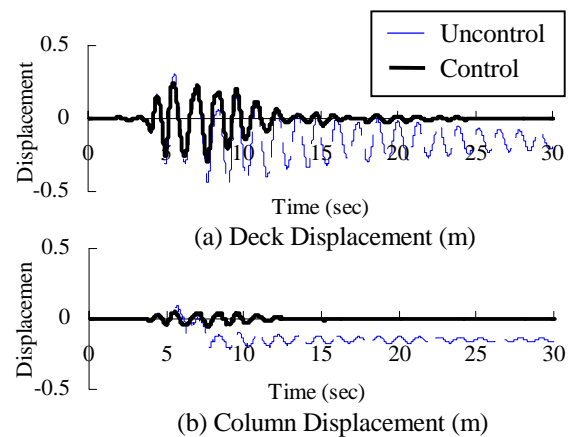
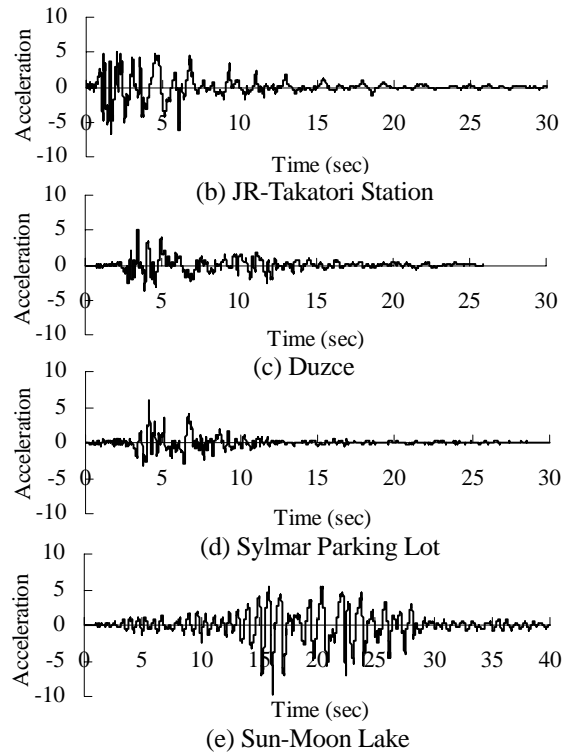


Figure 5 Displacements Responses under JMA Kobe

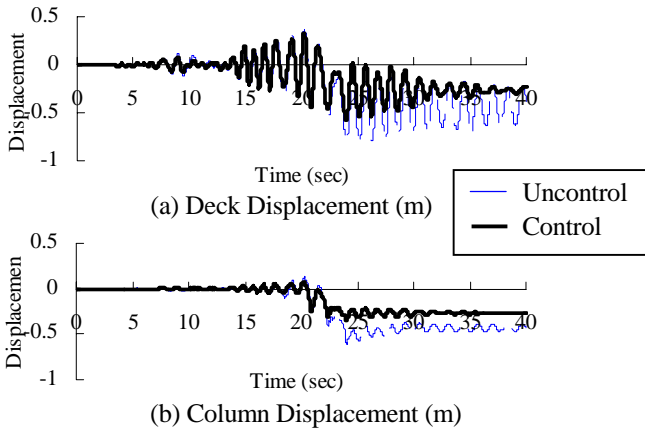


Figure 6 Displacements Responses under Sun-Moon Lake

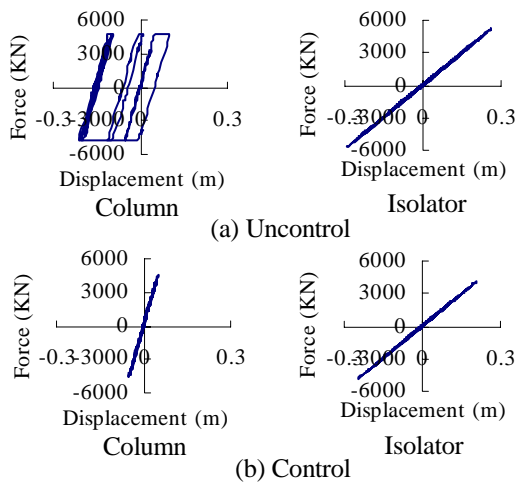


Figure 7 Hysteretic Loops under JMA Kobe

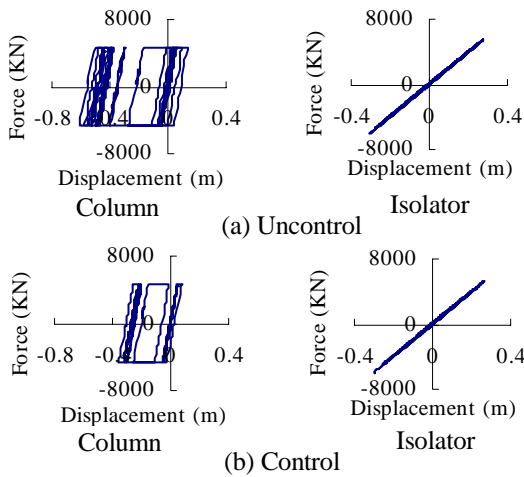


Figure 8 Hysteretic Loops under Sun-Moon Lake

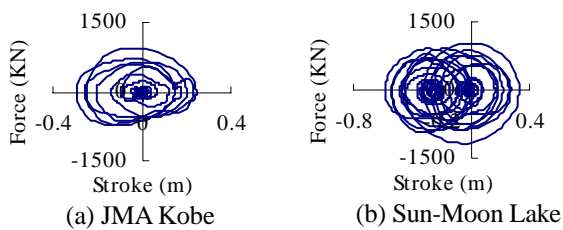


Figure 9 Damping Force v.s. Stroke Hystereses

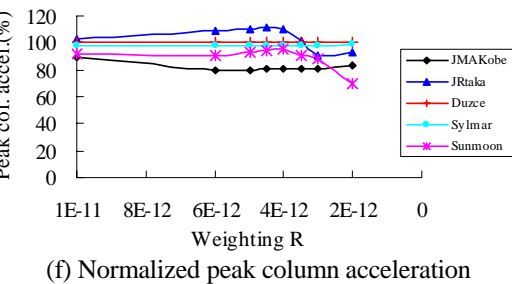
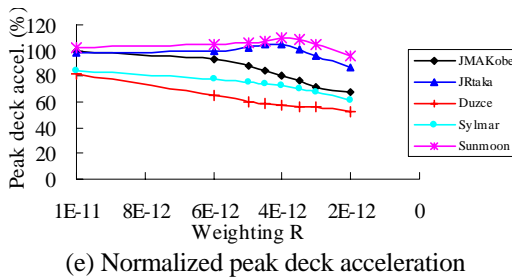
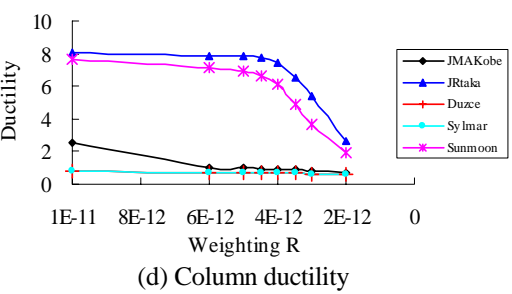
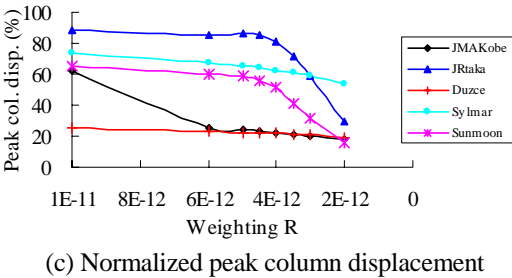
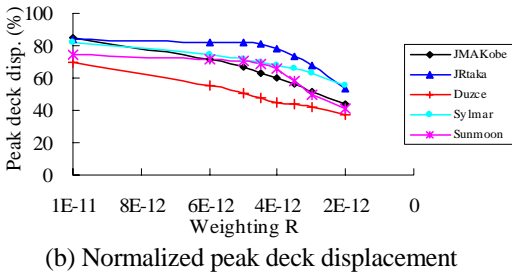
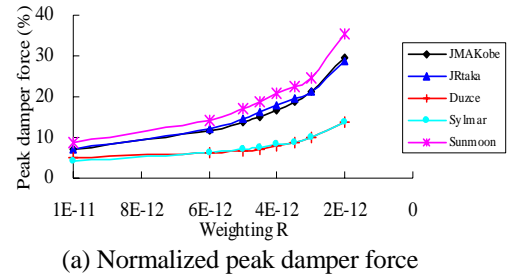


Figure 10 Performance Indices v.s. Weighting R of External Dampers under Five Excitations

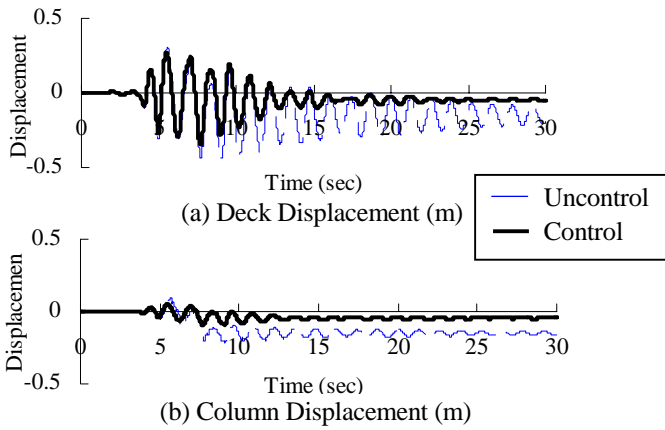


Figure 11 Displacements Responses under JMA Kobe

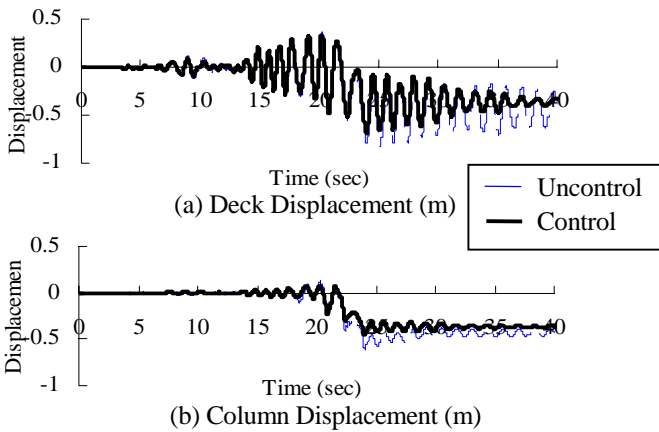


Figure 12 Displacements Responses under Sun-Moon Lake

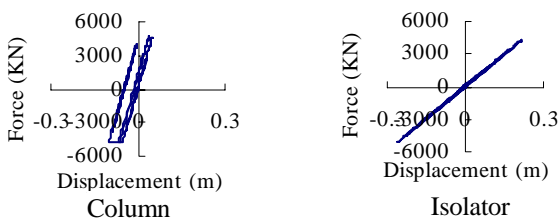


Figure 13 Hysteretic Loops under JMA Kobe

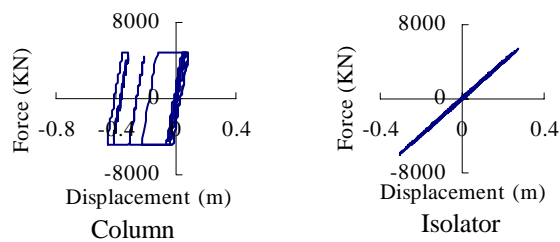


Figure 14 Hysteretic Loops under Sun-Moon Lake

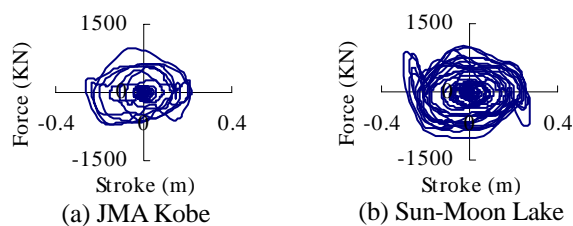
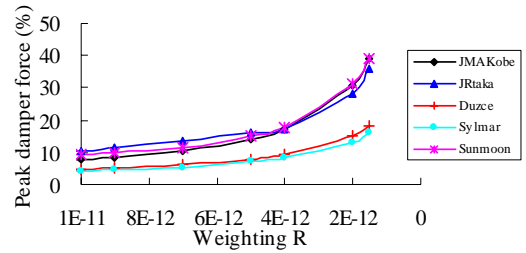
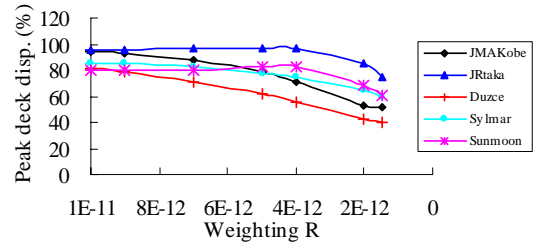


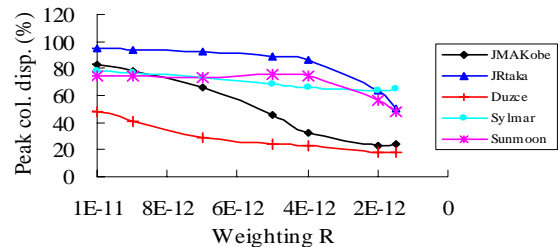
Figure 15 Damping Force v.s. Stroke Hystereses



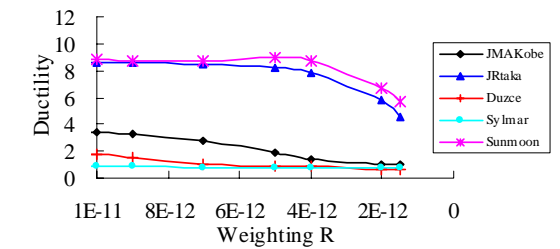
(a) Normalized peak damper force



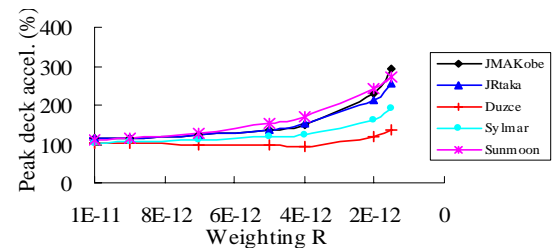
(b) Normalized peak deck displacement



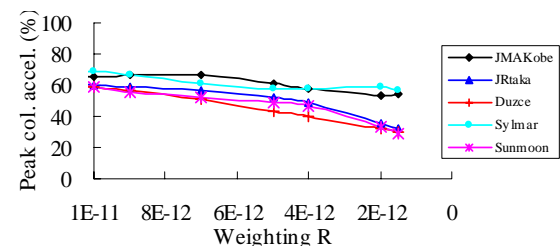
(c) Normalized peak column displacement



(d) Column ductility



(e) Normalized peak deck acceleration



(f) Normalized peak column acceleration

Figure 16 Performance Indices v.s. Weighting R of Internal Dampers under Five Excitations